The Global Climate in 2015–2019

WEATHER CLIMATE WATER

WORLD METEOROLOGICAL ORGANIZATION

Chairperson, Publications Board
World Meteorological Organization (WMO)
7 bis, avenue de la Paix
P.O. Box 2300
CH-1211 Geneva 2, Switzerland

Tel.: +41 (0) 22 730 84 03
Fax: +41 (0) 22 730 81 17
Email: publications@wmo.int

The *Global Climate in 2015–2019* is part of the WMO Statements on Climate providing authoritative information on the state of the climate and impacts. It builds on operational monitoring systems at global, regional and national scales. It has been authored by: Peter Siegmund, lead author (Royal Netherlands Meteorological Institute), Jacob Abermann (University of Graz, Austria), Omar Baddour (WMO), Pep Canadell (CSIRO Climate Science Centre, Australia), Anny Cazenave (Laboratoire d'Etudes en Géophysique et Océanographie Spatiales, Centre National d'Etudes Spatiales and Observatoire Midi-Pyrénées, France), Chris Derksen (Environment and Climate Change Canada), Arthur Garreau (Météo-France), Stephen Howell (Environment and Climate Change Canada), Matthias Huss (ETH Zürich), Kirsten Isensee (IOC-UNESCO), John Kennedy (UK Met Office), Ruth Mottram (Danish Meteorological Institute), Rodica Nitu (WMO), Selvaraju Ramasamy (Food and Agriculture Organization of the United Nations), Katherina Schoo (IOC-UNESCO), Michael Sparrow (WMO), Oksana Tarasova (WMO), Blair Trewin (Bureau of Meteorology, Australia), Markus Ziese (Deutscher Wetterdienst)

Cover illustration: Adobe Stock, Frédérique Julliard

Contents

THE GLOBAL CLIMATE 2015–2019

GLOBAL TEMPERATURE RISE

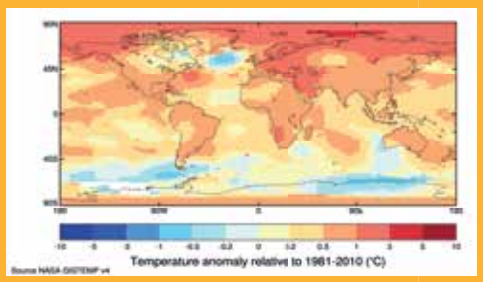

Global five-year average temperature anomalies (relative to 1981–2010) for 2015– 2019. Data are from NASA GISTEMP v4. Data for 2019 to June 2019.

2015–2019
- Warmest five-year period
- 0.2 °C higher than 2011–2015

2016
- Is the warmest year on record, over 1 °C higher than pre-industrial period

GREENHOUSE GAS CONCENTRATIONS INCREASE

Global mean surface concentrations 2015–2017

- CO_2 403 parts per million
- N_2O 329 parts per billion
- CH_4 1852 parts per billion

OCEAN ACIDIFICATION

Ocean acidity increasing due to rising CO_2

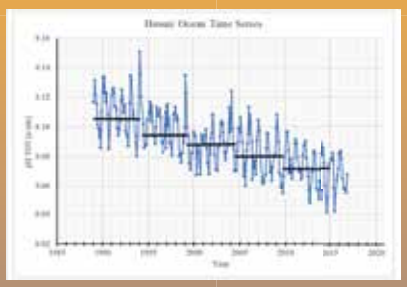

pCO_2 and pH records from three long-term ocean observation stations. Credit: IOC-UNESCO, NOAA-PMEL, IAEA OA-ICC.

OCEAN WARMING

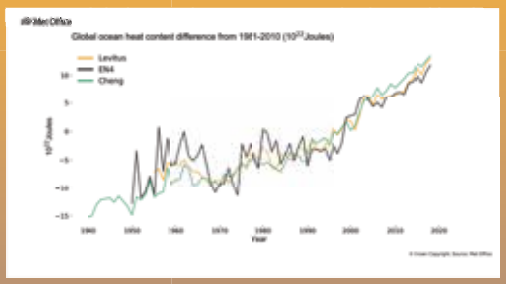

Source: NOAA NCEI, UK Met Office, IAP.

SEA LEVEL CONTINUES TO RISE

Global sea level continued to rise
Ice melt major contributor

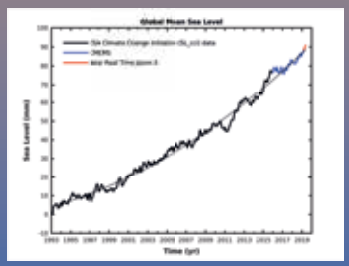

Data source: European Space Agency (ESA) Climate Change Initiative (CCI) sea level data until December 2015,extended by data from the Copernicus Marine Service (CMEMS) as of January 2016

CRYOSPHERE

Ice melt is an indicator of global warming.

Arctic

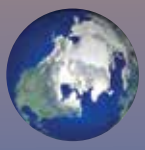

Arctic average summer minimum and winter maximum sea-ice extents were well below the 1981–2010 average every year from 2015 to 2019.

Antarctic

Antarctic experienced its lowest and second lowest summer sea-ice extent in 2017 and 2018, respectively.

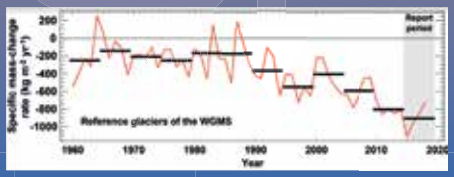

Average of observed annual specific mass-change rate of all World Glacier Monitoring Service (WGMS) reference glaciers,including pentadal means.

EXTREME EVENTS

Mortality and economic losses

2017
>2 000 DEATHS
attributed to Hurricane *Maria*, Puerto Rico and Dominica

2015–2019
>8 900 DEATHS
attributed to heatwaves worldwide

2017
>US$ 125 billion
Economic losses attributed to Hurricane *Harvey*

Large-scale heat extremes attributable to human influence

2016
>US$ 16 billion
Economic losses attributed to the wildfires in California

Executive summary

Compared to the previous five-year assessment period 2011–2015, the current five-year period 2015–2019 has seen a continued increase in carbon dioxide (CO_2) emissions and an accelerated increase in the atmospheric concentration of major greenhouse gases (GHGs), with growth rates nearly 20% higher. The increase in the oceanic CO_2 concentration has increased the ocean's acidity.

The five-year period 2015–2019[1] is likely to be the warmest of any equivalent period on record globally, with a 1.1 °C global temperature increase since the pre-industrial period and a 0.2 °C increase compared to the previous five-year period.

Continuing and accelerated trends have also predominated among other key climate indicators, including an acceleration of rising sea levels, a continued decline in the Arctic sea-ice extent, an abrupt decrease in Antarctic sea ice, continued ice mass loss in the glaciers and the Greenland and Antarctic ice sheets, and the clear downward trend in the northern hemisphere spring snow cover.

More heat is being trapped in the ocean; 2018 had the largest ocean heat content values on record measured over the upper 700 meters. Precipitation has increased in some regions and decreased in others. Heatwaves were the deadliest meteorological hazard in the 2015–2019 period, affecting all continents and resulting in new temperature records in many countries accompanied by unprecedented wildfires that occurred in particular in Europe, North America and other regions. The 2019 northern summer saw record-breaking wildfires that expanded to the Arctic regions, setting new records, and wide-spread fires in the Amazon rainforest.

Among all weather-related hazards, tropical cyclones were associated with the largest economic losses, with floods, landslides and associated loss and damage. The costliest hazard event was *Hurricane Harvey* in 2017, which led to an estimated economic loss of more than US$ 125 billion.

Climate-related risks associated with climate variability and change exacerbated food insecurity in many places, in particular Africa due to the impact of drought, which increased the overall risk of climate-related illness or death. Higher sea-surface temperatures endangered marine life and ecosystems. Higher temperatures threaten to undermine development through adverse impacts on gross domestic product (GDP) in developing countries.

[1] For 2019 only six months of data are currently available.

Key findings

GREENHOUSE GASES

CO_2 EMISSIONS AND GHG CONCENTRATIONS INCREASED

CO_2 is responsible for about 66% of the total radiative forcing from long-lived GHGs since pre-industrial time, with methane (CH_4) responsible for about 17% and nitrous oxide (N_2O) for 6%. The global budget of anthropogenic carbon has continued to grow since 2015 due to the increase in CO_2 emissions from the combustion of fossil fuels (coal, oil and gas) and cement production. CO_2 emissions from 2015 to 2019 are estimated to be at least 207 Gt CO_2, exceeding the 200 Gt CO_2[2] emitted during the previous five-year period of 2010–2014. Sinks for CO_2 are distributed across the hemispheres, on land and oceans, but CO_2 fluxes in the tropics (30°S–30°N) are close to carbon neutral due to the CO_2 sink being largely offset by emissions from deforestation. Sinks for CO_2 in the southern hemisphere are dominated by the removal of CO_2 by the oceans, while the stronger sinks in the northern hemisphere have similar contributions from both land and oceans.

The latest analysis of observations from the WMO Global Atmosphere Watch shows that globally averaged surface concentrations calculated from this in-situ network for CO_2, CH_4 and N_2O reached new highs (Figure 1). The growth rates of the CO_2, CH_4 and N_2O concentrations in the atmosphere averaged over the 2015–2017 period for which data have been completed and processed are each about 20% higher than those over 2011–2015 (Table 1).[3] Preliminary analysis shows that in 2018 the CO_2 annual mean concentration at Mauna Loa Observatory, Hawaii, reached 408.52 ppm and the increase from 2017 to 2018 was 1.97 ppm. From January to August 2019 the increase in the concentration (deseasonalized trend) was 0.85 ppm.

Table 1. Concentrations of CO_2 (ppm), CH_4 (parts per billion, ppb) and N_2O (ppb), their growth rates (ppm/year for CO_2, ppb/year for CH_4 and N_2O) averaged over 2015–2017 and 2011–2015, the relative change in growth rates between 2011–2015 and 2015–2017, and the percentage of 2015–2017 concentration to pre-industrial concentration (before 1750). *Source: WMO Global Atmosphere Watch*

	Concentration			*Growth rate*		
	2015-2017	*2011-2015*	*2015-2017 % to pre-industrial*	*2015-2017*	*2011-2015*	*% change*
CO_2	403	395.5	145	2.6	2.2	+18%
CH_4	1851.7	1826.4	256	8.7	7.2	+21%
N_2O	329.1	326.2	122	0.87	0.73	+19%

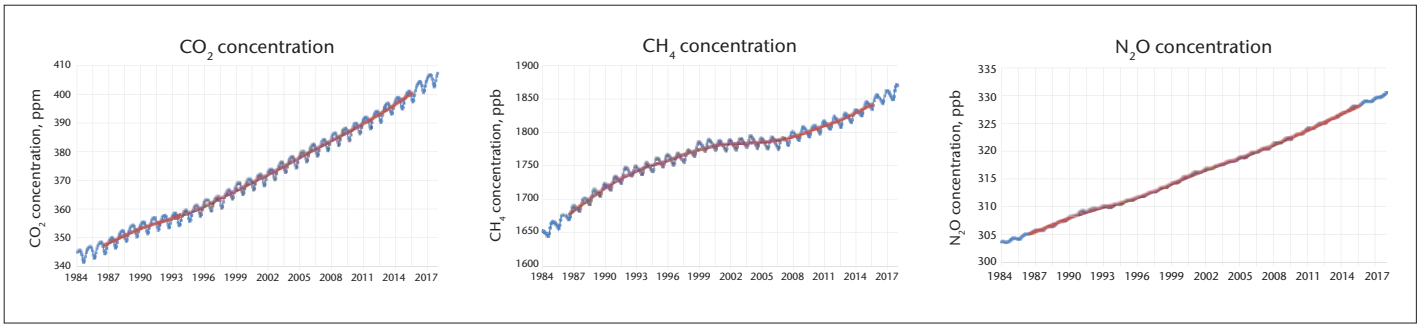

Figure 1. Time series of globally averaged concentrations of CO_2 in ppm (left), CH_4 in ppb (middle) and N_2O in ppm (right). Blue lines are monthly mean global averaged concentrations, red lines are five-year running averaged monthly mean concentrations. *Source: WMO Global Atmosphere Watch*

[2] 1 gigaton = 1 billion tons.

[3] The current growth rate of CO_2 of 2.6 ppm/year corresponds to a mass of about 50 kg CO_2 per person per week worldwide.

TEMPERATURE

GLOBAL TEMPERATURE CONTINUES TO RISE, 2015–2019 IS SET TO BE WARMEST FIVE-YEAR PERIOD

The years 2015 to 2018 were the four warmest years on record and 2019, although only six months of data are currently available, will likely join them as one of the five warmest years – most likely second or third warmest – if temperature anomalies continue at the current high levels to the end of the year. The average global temperature for 2015–2019, which is currently estimated to be 1.1 ± 0.1 °C above pre-industrial (1850–1900) level, is therefore likely to be the warmest of any equivalent period on record. It is 0.20 ± 0.08 °C warmer than the average for 2011–2015 (Figure 2).

Continental average temperatures typically show greater variability than the global mean. Even so, five-year average temperatures for 2015–2019 are currently the warmest or second warmest on record for each of the inhabited continents (Figure 3). Figure 4 shows a map of temperature anomalies for 2015–2019 relative to the long-term average for 1981–2010.

The global mean land-surface air temperature[4] for 2015–2019 was approximately 1.7 °C above pre-industrial and 0.3 °C warmer than 2011–2015. Nearly all land areas were warmer than average, with only a few exceptions: an area of Canada and an area of the Antarctic in the Indian Ocean sector. The five-year average temperatures were the highest on record for large areas of the United States including Alaska, eastern parts of South America, most of Europe and the Middle East, northern Eurasia, Australia, and areas of Africa south of the Sahara.

The global mean sea-surface temperature for 2015–2019 was approximately 0.8 °C above pre-industrial and 0.13 °C warmer than 2011–2015. Over the oceans, below-average sea-surface temperatures were observed to the south of Greenland (one of the few areas globally to have seen long-term cooling), the eastern Indian Ocean, an area off the coast of West Africa, some areas of the South Atlantic, the Drake Passage and an area of the Southern Ocean in the Pacific sector. Other areas were mostly warmer than average. Record warmth was recorded over areas of the north-east Pacific, the western North Atlantic, the western Indian Ocean, areas of the South Atlantic, and the Tasman Sea, which has seen a number of severe marine heatwaves in the past five years.

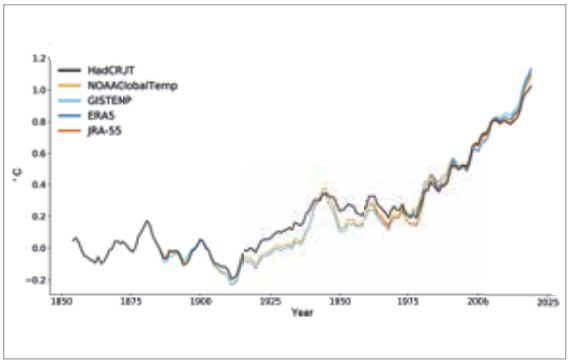

Figure 2. Five-year running average of global temperature anomalies (relative to pre-industrial) from 1854 to 2019 for five datasets: HadCRUT.4.6.0.0, NOAAGlobalTemp v5, GISTEMP v4, ERA5 and JRA-55. Data for 2019 to June. The anomalies are monthly anomalies averaged to years.

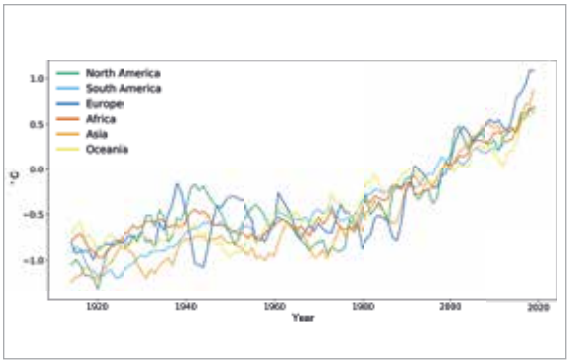

Figure 3. Five-year running average of continental-scale temperature anomalies (relative to 1981–2010) from 1910 to 2019 for North America, South America, Europe, Africa, Asia and Oceania. Data are from NOAA. Data for 2019 to June. The anomalies are monthly anomalies averaged to years.

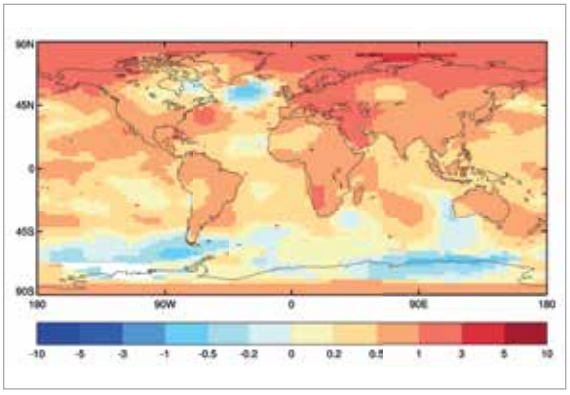

Figure 4. Five-year average temperature anomalies relative to the 1981–2010 average. Data are from National Aeronautics and Space Administration (NASA) GISTEMP v4. Data for 2019 to June. The anomalies are monthly anomalies averaged to years.

[4] The global temperature assessment is based on five datasets: HadCRUT.4.6.0.0 (UK Met Office Hadley Centre and Climatic Research Unit, University of East Anglia), GISTEMP v4 (National Aeronautics and Space Administration Goddard Institute for Space Studies), NOAAGlobalTemp (National Oceanic and Atmospheric Administration (NOAA), National Centers for Environmental Information (NCEI), ERA5 (European Centre for Medium-range Weather Forecasts), and JRA-55 (Japan Meteorological Agency).

OCEAN

SEA-LEVEL RISE IS ACCELERATING

Sea level continues to rise at an accelerated rate as shown by altimeter satellites. The total elevation of the global mean sea level over the altimetry era (since January 1993) has reached 90 mm. Figure 5 shows the altimetry-based global mean sea-level time series for the period January 1993–May 2019. Superimposed to the long-term trend (highlighted by the thin black curve in Figure 5), temporary positive or negative deviations are related to El Niño and La Niña events, for example in 1997/98, 2011, 2015/16. Sea level has continued to rise during recent years. Over the five-year period 2014–2019, the rate of global mean sea-level rise has amounted to 5 mm/year.[5] This is substantially faster than the average rate since 1993 of 3.2 mm/year.

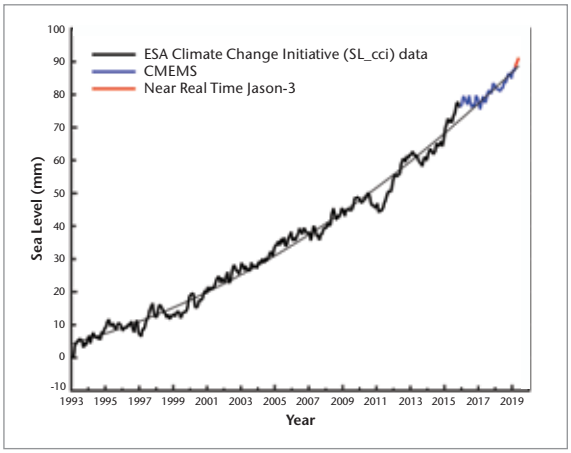

Figure 5. Time series of altimetry-based global mean sea level for the period January 1993–May 2019. The thin black line is a quadratic function showing the mean sea-level rise acceleration. Data source: European Space Agency Climate Change Initiative sea-level data until December 2015, extended by data from the Copernicus Marine Service as of January 2016 and near-real-time Jason-3 as of April 2019

The observed rate of global mean sea-level rise has increased from 3.04 mm/year during the 10-year period 1997–2006 to 4.36 mm/year during the previous 10-year period 2007–2016 (Figure 6). The sea-level budget for the period 1993–2016 is closed to within 0.3 mm/year. The contribution of land ice melt from the world glaciers and ice sheets has increased over time and now dominates the sea-level budget (World Climate Research Programme Sea Level Budget Group, 2018).

MORE HEAT BEING TRAPPED IN THE OCEAN

The capacity of the ocean to absorb heat is a critical part of the climate system. It is estimated that more than 90% of the radiative imbalance associated with anthropogenic climate change is taken up by the oceans. Over the last 15 years, new observation systems, especially the Argo series of floats, have allowed systematic near-global monitoring of ocean heat content. Prior to 2005, sampling was more infrequent and more widely spaced, and uncertainties in ocean heat content estimates are, therefore, much larger.

Ocean heat content has reached new records since 2015. Measured over the layer from the surface to 700 meters depth (Figure 7), 2018 had the largest ocean heat content values on record, with 2017 ranking second and 2015 third. 2016 also had higher values than any pre-2015 year in most datasets. In the NCEI

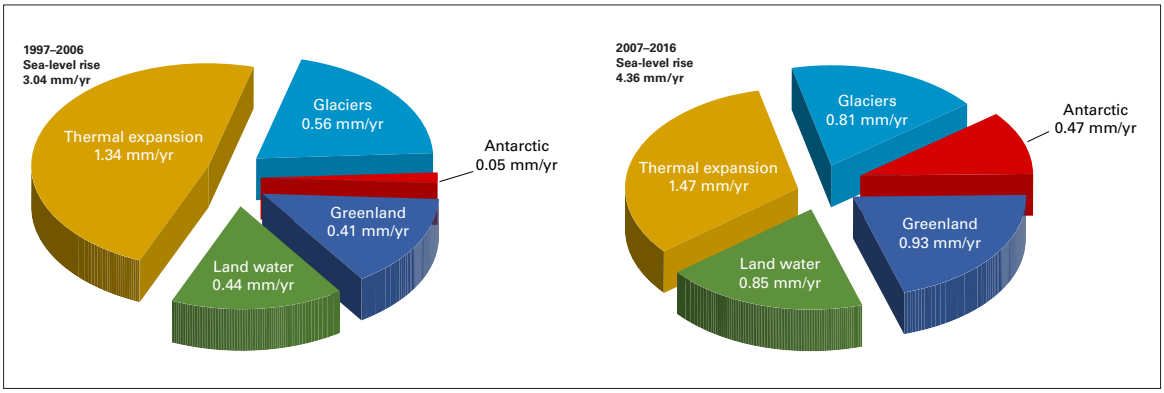

Figure 6. Contributions by different components to the rate of global mean sea-level rise during the periods 1997–2006 (left) and 2007–2016 (right). Data source: European Space Agency Sea Level Budget Closure Project (v2 version). The observed rates of global mean sea-level rise are shown in the upper left corners. The difference between the sum of the various contributions and the observed values indicates errors in some of the components or contributions from components missing in the sea level budget computation.

[5] The current rate of global mean sea-level rise of 5 mm/year corresponds to a volume of water discharged by the Amazon river in about 3 months.

dataset, the ocean heat content anomaly (recomputed relative to the reference period 1981–2010) for 2018 was 13.0 x 10^{22} J for the 0–700 meter layer, and 18.2 x 10^{22} J for the 0–2000 meter layer, compared with the pre-2015 annual records of 9.5 x 10^{22} J and 14.3 x 10^{22} J, respectively.[6]

SEAWATER IS BECOMING MORE ACID

The ocean absorbs around 30% of the annual emissions of anthropogenic CO_2 to the atmosphere, thereby helping to alleviate the impacts of climate change on the planet. The ecological costs to the ocean, however, are high, as the absorbed CO_2 reacts with seawater and changes the acidity of the ocean. This decrease in seawater pH is linked to shifts in other carbonate chemistry parameters, such as the saturation state of aragonite, the main form of calcium carbonate used for the formation of shells and skeletal material. Observations from open ocean sources over the last 20 to 30 years have shown a clear trend of decreasing average pH, caused by increased concentrations of CO_2 in seawater (Figure 8). Trends of ocean acidification in coastal locations are more difficult to assess, due to the highly dynamic, highly variable coastal environment affected by temperature change, freshwater runoff, nutrient influx, biological activity and large ocean oscillations. There has been an overall increase in acidity of 26% since the beginning of the industrial revolution.

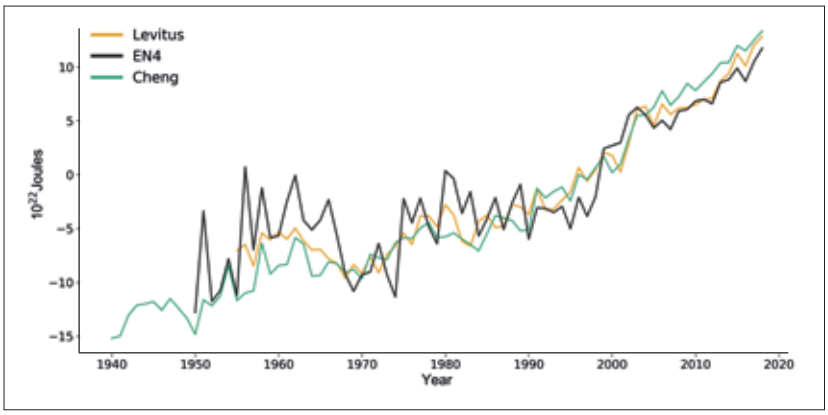

Figure 7. Global ocean heat content change (x 10^{22} J) for the 0–700-meter layer relative to the 1981–2010 baseline. The lines show annual means from the Levitus analysis produced by NOAA NCEI, the EN4 analysis produced by the UK Met Office Hadley Centre, and the Institute of Atmospheric Physics ocean analysis (Cheng et al., 2019).

CRYOSPHERE

SEA-ICE EXTENT CONTINUES TO DECREASE

For all years from 2015 to 2018, the Arctic's average September minimum (summer) sea-ice extent[7] was well below the 1981–2010 average. Arctic sea-ice extent for July 2019 set a new record low. Average summer sea-ice extent during 2015–2018 was less variable compared to 2011–2015 when the record low summer sea-ice extent occurred in 2012. 2015–2018 was marked by a considerable retreat of the Arctic sea-ice extent towards the Central Arctic particularly prominent in the Beaufort and Chukchi Seas. The long-term trend over 1979–2018 indicates that the summer sea-ice extent in the Arctic has declined at a rate of approximately 12% per decade.

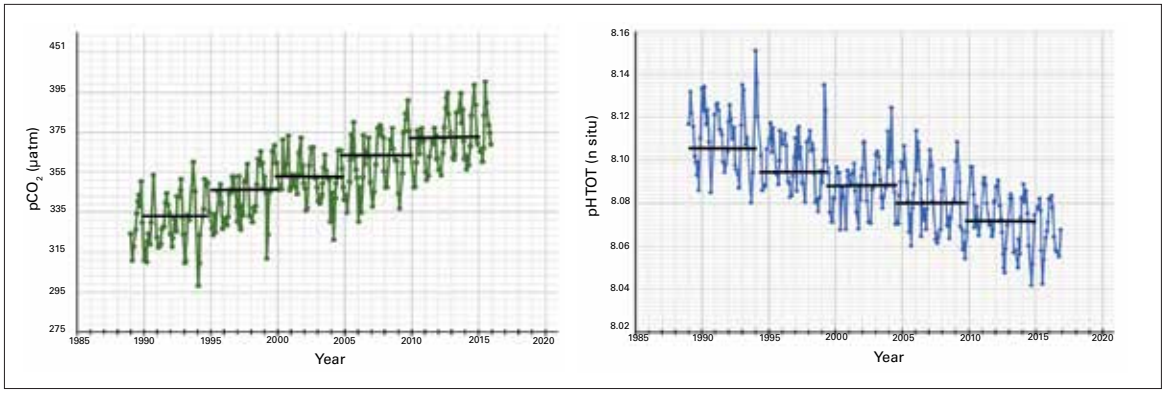

Figure 8. pCO_2 and pH record for the Hawaii Ocean Time-Series in the Pacific Ocean, with five-year running average pCO_2 and pH indicated by black bars. *Source: Intergovernmental Oceanographic Commission of UNESCO (IOC-UNESCO), NOAA Pacific Marine Environmental Laboratory, International Atomic Energy Agency Ocean Acidification International Coordination Centre*

[6] The current increase rate of the world's ocean heat content in the 0–2000-meter layer is about 1 x 10^{22} joules/year. This is about 20 times as much as the world's annual primary energy consumption, which in 2017 was 13 511 million tons of oil equivalent (BP, 2018), or 0.05 x 10^{22} joules.

[7] Sea-ice extent is defined as the area covered by sea ice that contains an ice concentration of 15% or more.

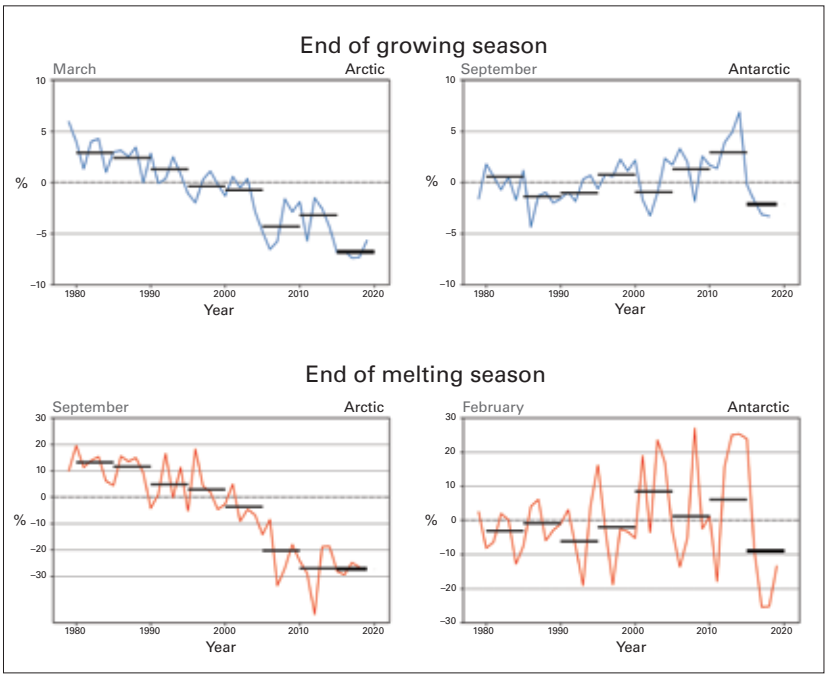

Figure 9. Time series of sea-ice extent anomalies (%) for the Arctic in March and Antarctic in September (maximum ice extent), and for the Arctic in September and Antarctic in February (minimum ice extent), relative to the 1981–2010 mean. Black bars indicate five-year averages. *Source: Sea Ice Index, Version 3 (Fetterer et al., 2017)*

The Arctic's average March maximum (winter) sea-ice extent has also declined over the 1979–2019 period at a rate of approximately 2.7% per decade. The average winter sea-ice extent was lower for 2015–2019 compared to 2011–2015. For all years from 2015–2019, the average winter sea-ice extent was well below the 1981–2010 mean, and the four lowest records for winter occurred in these five years. The largest retreat of the sea-ice extent for 2015–2019 has occurred in the Barents and Bering Seas.

In Antarctica, a remarkable feature of 2015–2019 for both the February minimum (summer) and September maximum (winter) has been that sea-ice extent values have become well below the 1981–2010 average since 2016. This is in considerable contrast to the previous 2011–2015 period and the longer-term 1979–2018 period that exhibited increasing trends in both seasons. During 2015–2019, the summer sea ice reached its lowest and second lowest extent on record in 2017 and 2018, respectively, with 2017 also being the second lowest winter extent. For most years from 2015–2019, the sea-ice extent retreat has been predominantly located in the Ross Sea in summer and in the Ross and Weddell Seas in winter.

ICE SHEETS CONTINUE LOSING MASS

The Greenland ice sheet has undergone significant changes over recent decades. While the overall ice mass was rather stable between 1981 and 2010, an accelerated loss of ice has been observed since the turn of the millennium. Figure 10 gives an indication of the regional distribution of average surface–mass balance (SMB) for the reference period 1986–2005 (left), the anomaly of the 2015–2018 period (middle) and 2018–2019 (right).[8] While most of the interior of Greenland actually gained a small amount of mass, strong mass loss occurred at the margins. In the dry north-east interior of Greenland no significant mass change occurred. Negative anomalies in the years 2015–2018 particularly occurred over large parts of the west coast ablation zone, while south-east Greenland's margin showed a mass change that was more positive than the 1981–2010 average. This pattern also occurred

[8] While SMB is measured directly in only a few locations around the ice sheet, SMB is shown here calculated from computer models. The reference periods are based on output from a high-resolution regional climate model (HIRHAM5) driven by climate reanalysis on the boundaries, and the most recent year is based on output from a weather forecasting model (HARMONIE-AROME) with full observational data assimilated.

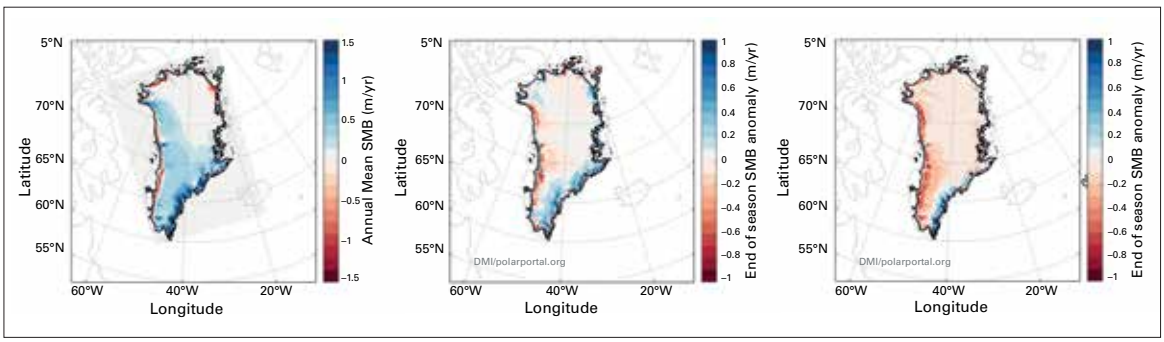

Figure 10. Average SMB for the reference period 1986–2005 (left), the anomaly for 2015–2018 (middle) and the end-of-season SMB for 2018–2019 (right). *Source: DMI/polarportal.dk*

for the season 2018/19 (right), when only the most south-eastern part of the country ended with a positive SMB anomaly. The other parts of Greenland, including the interior of the ice sheet, showed a notable negative SMB anomaly that is strongly correlated with the exceptional summer heatwave that peaked in Greenland in early August, producing runoff from the ice sheet of up to 11 billion tons per day.[9]

The amount of ice lost annually from the Antarctic ice sheet increased at least six-fold between 1979 and 2017. The total mass loss from the ice sheet increased from 40 Gt per year in 1979–1990 to 252 Gt per year in 2009–2017. The contribution to sea-level rise from Antarctica averaged 0.36 ± 0.05 mm per year with a cumulative 14.0 ± 2.0 mm since 1979. Most of the ice loss takes place by melting of the ice shelves[10] from below, due to incursions of relatively warm ocean water, especially in west Antarctica and to a lesser extent along the peninsula and in east Antarctica.

GLACIERS UNDERGO RECORD MASS LOSS

Variations in glacier mass are mainly affected by summer air temperatures, solid precipitation and solar radiation. Long-term cumulative glacier mass changes are thus a valuable indicator integrating the effects of various components of the global climate system on snow and ice.

For the period 2015–2018, data from the World Glacier Monitoring Service reference glaciers indicate an average specific mass change of –908 mm water equivalent per year. This is more negative than in all other five-year periods since 1950, including the previous five-year period (2011–2015) (Figure 11).

Global mass change estimates require extrapolation of the scattered direct observations to all glaciers. An assessment at the global scale (Zemp et al., 2019) indicates an acceleration of glacier mass loss rate since 1985 after moderately negative values. Over the last decade, glaciers lost more than 300 Gt per year on average, leading to a contribution to sea-level rise of about 0.8 mm per year.

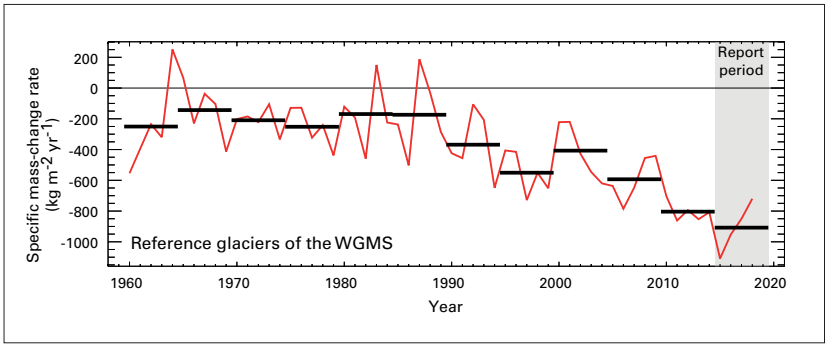

Figure 11. Time series of average of observed annual specific mass-change rate of all World Glacier Monitoring Service reference glaciers, including five-year averages

SPRING SNOW COVER DECREASED

Northern hemisphere spring snow cover is found across high-elevation, subarctic, and Arctic land areas. Snow-cover extent trends over 1967–2018 are –4.2 ± 1.5% per decade for May and –12.9 ± 3.6% per decade for June (Figure 12). Approximately 800 000 km2 of northern hemisphere spring snow cover has been lost per degree Celsius in observed extratropical continental warming. While there are small reductions during the autumn and winter, seasonal snow loss is dominated by changes in May and June. Although May and June snow-cover extent during the seasons of 2017 and 2018 were near or above historical averages, the snow loss during 2011–2015 and 2015–2018 exceeded the reductions over the longer 2000–2018 period.

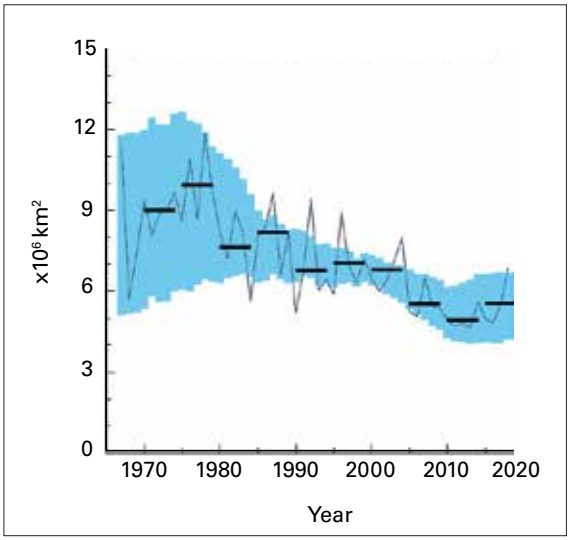

Figure 12. Time series of northern hemisphere snow-cover extent in June, from 1967 to 2018, including five-year averages. Shading represents uncertainty based on spread among the following five component datasets: (1) NOAA Rutgers CDR, Estilow et al., 2015; (2) GlobSnow version 2.0, Takala et al., 2011; (3) MERRA-2, Reichle et al., 2017; (4) Crocus snowpack model driven by ERA-Interim, Brun et al., 2013; (5) temperature index model driven by ERA-Interim, Brown et al., 2003. *Source: Environment and Climate Change Canada*

[9] This corresponds to about 0.6 times the discharge of the Amazon river.

[10] Ice shelves are floating sheets of ice permanently attached to a land mass.

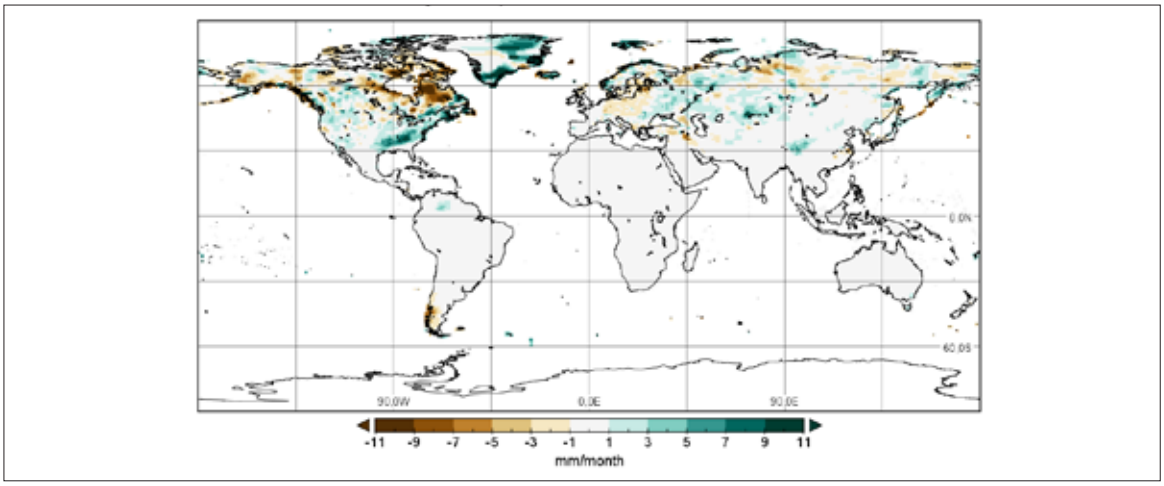

Figure 13. Anomaly of the water equivalent of snow from January 2015 to March 2019 with reference to the long-term means 1982–2010 based on the Global Precipitation Climatology Centre (GPCC) Monitoring Product V6 (DOI: 10.5676/DWD_GPCC/MP_M_V6_100). *Source: GPCC, Deutscher Wetterdienst, Germany*

The water equivalent of solid precipitation, which is mainly snow in the local winter season, computed as the product of the monthly precipitation total and fraction of solid precipitation is shown in Figure 13. Above-average snowfall was observed in eastern Europe and eastern United States, while Canada received below-average snowfall. Central Europe and southern South America received less than normal snow. Negative anomalies can be caused by less total precipitation and by a lower fraction of snow, which can lead to reduced water availability by snowmelt in the warm season.

A comparison of the most recent five-year period with previous five-year periods (not displayed) shows that nearly all regions where snow occurs received more snow in the most recent period than in the previous ones, which can be explained by natural variability.

PRECIPITATION

PRECIPITATION INCREASES IN SOME PARTS AND DECREASES IN OTHERS

Precipitation totals from the 48-month period January 2015 to December 2018 were compared against different reference periods. Year-to-year variations can counterbalance positive and negative anomalies at a certain place.

Comparing the last four years 2015–2018 with the five-year period 2011–2015 shows that the average precipitation totals were higher in the latter period than in the former in large regions in southern South and North America, eastern Europe and most of Asia (Figure 14). In contrast, less precipitation fell in large parts of Europe, south-west and southern Africa, northern North America and a large part of South America, the Indian Monsoon region, and northern and western Australia.

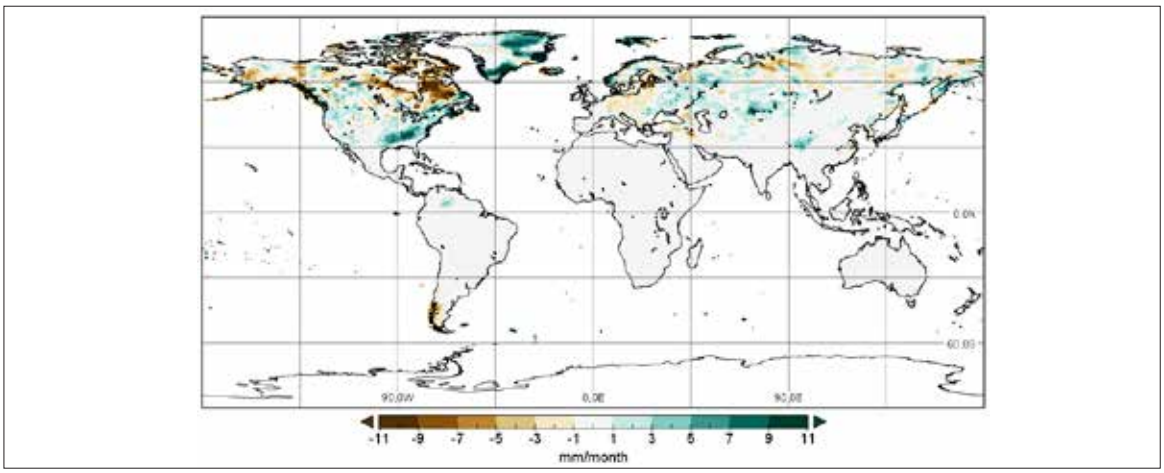

Figure 14. Difference in monthly average precipitation totals between 2015–2018 and 2011–2015. *Source: GPCC, Deutscher Wetterdienst, Germany*

Comparing short periods can exaggerate the effects of slowly varying circulation patterns such as the El Niño–Southern Oscillation (ENSO). Therefore, precipitation totals from January 2015 to December 2018 were compared to observed totals from 1951 to 2010. Large parts of the northern hemisphere received precipitation amounts rated in the wettest 20% (Figure 15). Some regions around the equator in Africa and Asia also received similarly rated totals, as well as the western interior of Australia and southern South America. In contrast, large regions with precipitation totals rated in the driest 20% were found in northern South America, southern and south-west Africa, the Indian Monsoon region and eastward of the Persian Gulf, Europe, Central and northern North America and north-east Australia.

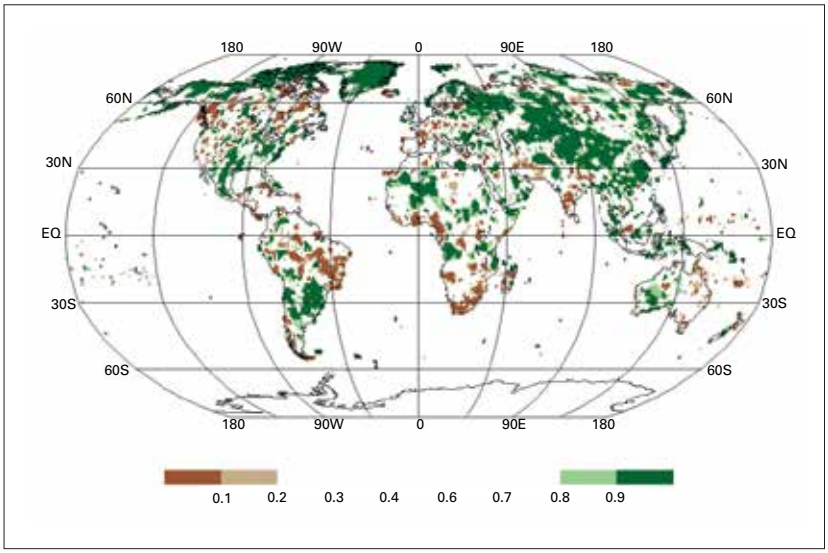

Figure 15. Total precipitation for 2015–2018 expressed as a percentile of the 1951–2010 reference period for areas that would have been in the driest 20% (brown) and wettest 20% (green) of the years during the reference period, with darker shades of brown and green indicating the driest and wettest 10%, respectively. *Source: GPCC, Deutscher Wetterdienst, Germany*

EXTREME EVENTS

DEADLY HEATWAVES AND COSTLY TROPICAL CYCLONES

Many of the major impacts of climate are associated with extreme events. These can be short-term events, such as tropical cyclones, or events that can extend over months or years such as droughts. Some extreme events bring substantial loss of life or population displacement, others may have limited casualties but major economic impacts. Figure 16 provides data on mortality and economic losses in the six WMO Regions associated with high-impact weather and climate events during the period 2015–2019 (to date).

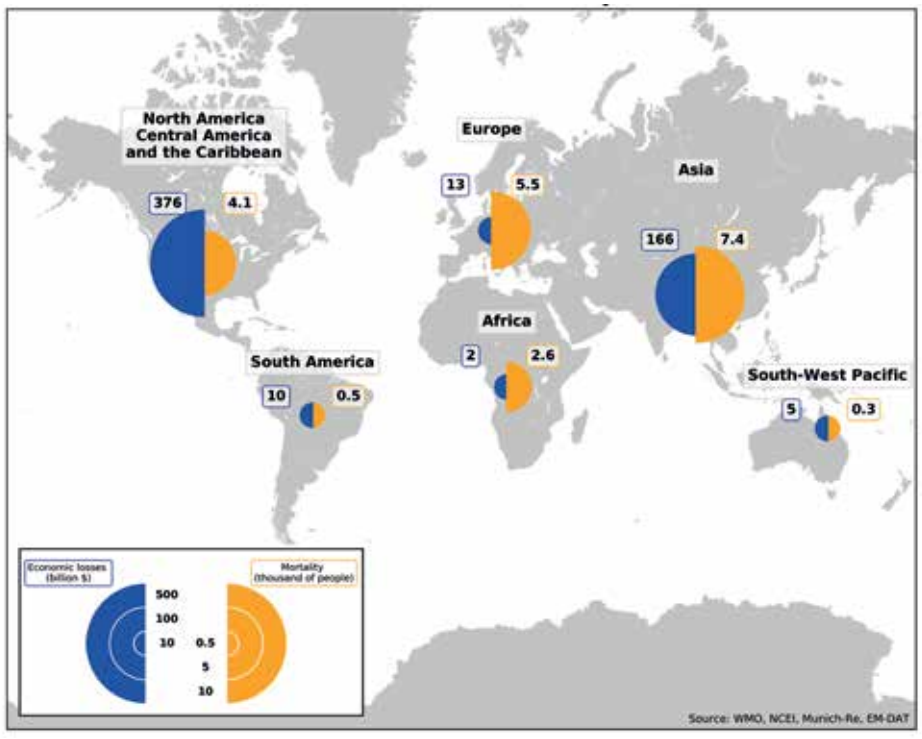

Figure 16. Mortality and economic losses associated with extreme weather in the period 2015–2019. The numbers apply to 88 extreme weather events, chosen based on mortality and economic losses. *Source: the NCEI Billion-dollar Weather and Climate Disasters list, the EM-DAT International Disaster Database, and the NatCatSERVICE of Munich Re*

Heatwaves have been the deadliest meteorological hazard in the 2015–2019 period, with wildfires also featuring especially in the Arctic, including Greenland, Alaska and Siberia, and in the Amazon forest. Summer 2019 saw unprecedented wildfires in the Arctic region. In June alone, these fires emitted 50 Mt of CO_2 into the atmosphere. This is more than was released by Arctic fires in the same month for the totality of the period 2010–2018.

The largest economic losses were associated with tropical cyclones. The 2017 Atlantic hurricane season was one of the most devastating on record, with more than US$ 125 billion in losses associated with Hurricane *Harvey* alone. In the Indian Ocean, in March and April 2019, unprecedented and devastating back-to-back tropical cyclones hit Mozambique.

High impact events from a mortality and economic point of view are described below, with lists of five most prominent events per type. The lists are chosen based on the impact and the geographical representativeness (Table 2).

TROPICAL CYCLONES

Overall, global tropical cyclone activity since 2015 has been close to the satellite-era average. The 2018 season was especially active, with the largest number of tropical cyclones of any year in the twenty-first century; all northern hemisphere basins had above-average activity, with the north-east Pacific having its largest accumulated cyclone energy (ACE) value on record. 2016 and 2017 were slightly below-average seasons globally, with the 2016/17 southern hemisphere season being amongst the least active of the satellite era, but both were active years in individual basins.

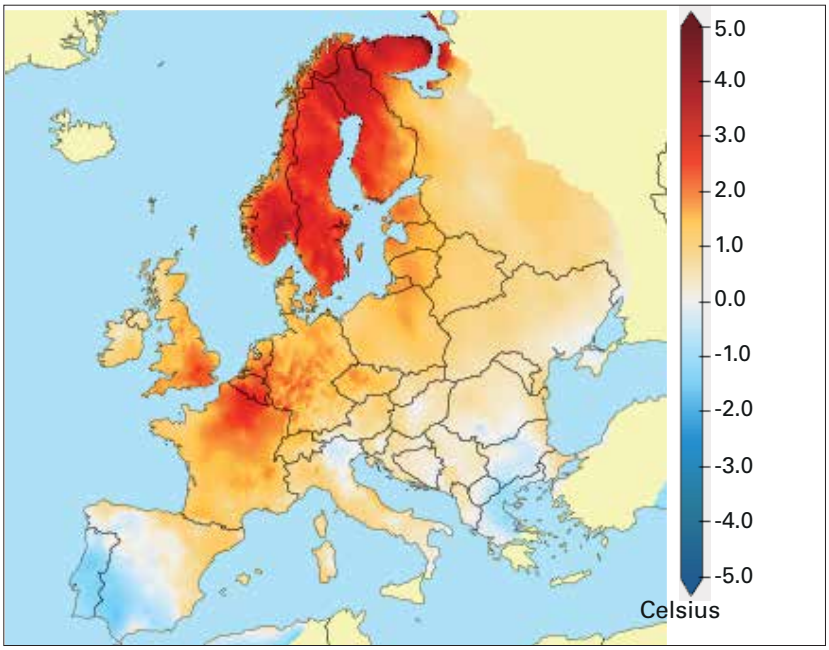

Figure 17. Europe experienced persistent high temperatures in late spring and summer 2018, as shown here for July. Data source: E-OBS. *Source: Copernicus Climate Change Service (C3S)/Royal Netherlands Meteorological Institute*

FLOODS

While tropical cyclones are responsible for many of the world's most destructive floods, there have been many other instances of major flooding since 2015. Some of these floods have been relatively long-lived responses to excessive rainfall in tropical regions during the monsoon season, but others have been shorter-term floods, including flash floods associated with intense rainfall over a few hours. Heavy rains have also contributed to major landslides in some parts of the world.

TORNADOES AND OTHER SEVERE LOCAL STORMS

During the last five years (to date), more than 300 losses of lives and economic losses of US$ 7.6 billion have been recorded globally as being associated with tornadoes, extratropical cyclones and hailstorms. In the United States, where data are updated regularly, overall tornado activity over the last five-year period has been close to average, with the 2017 season having above-average and the 2018 season below-average numbers. The 2019 season to date has been very active, with May 2019 having provisionally the second-largest number of tornadoes for any month after April 2011.

HEATWAVES

Extreme heat and heatwaves were recorded in many parts of the world during the period 2015–2019 (to date). Heatwaves have a

particularly high impact on human health and were responsible for the heaviest casualties of any severe weather or climate during the same period.

DROUGHT

Droughts have had major impacts, both humanitarian and economic, in numerous parts of the world since 2015. Significant droughts occurred on all inhabited continents (Figure 18 shows rainfall deficiency for Australia), but some of the largest impacts were in Africa, where millions of people required assistance after food shortages, and significant numbers were displaced.

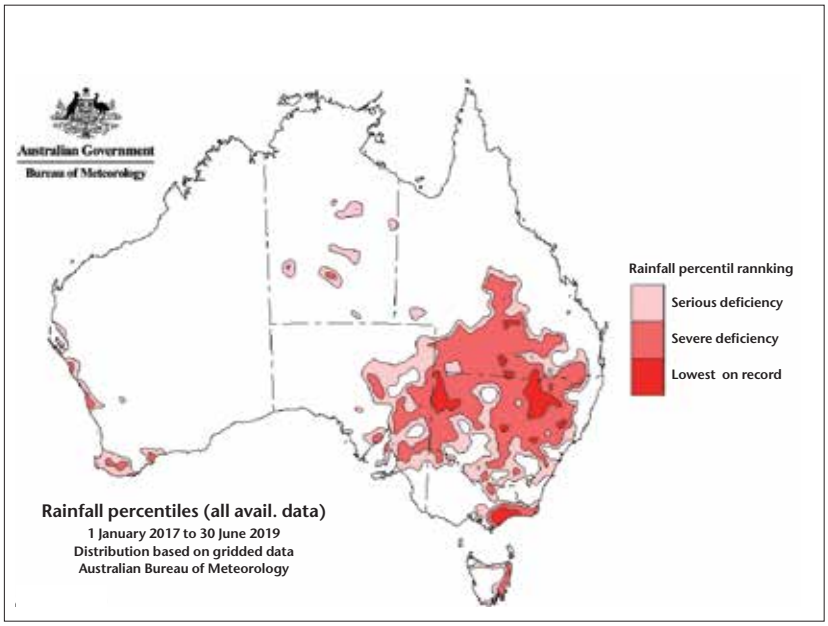

Figure 18. Rainfall deficiency for Australia for the period January 2017–June 2019. *Source: Australian Bureau of Meteorology*

WILDFIRES

While not strictly a weather phenomenon, wildfires are strongly influenced by weather and climate phenomena. Drought substantially increases the risk of wildfire in most forest regions (although it can reduce the risk of grassland fires, due to lack of fuel), with a particularly strong influence on long-lived fires. The three largest economic losses on record from wildfires have all occurred in the last four years. In 2019 there were unprecedented wildfires in the Arctic and widespread fires in the Amazon rainforest, with dramatic environmental impacts.

COLD EVENTS

Despite higher temperatures overall, there were numerous significant cold events and snowfalls over the last five years. Many of these occurred in North America.

Figure 19. Smoke plume from the Camp Fire in California, November 2018. *Source: NASA Earth Observatory*

Table 2. List of five prominent events by types during 2015–2019, with date and locations where impacts were recorded

Tropical cyclone
October 2016, North Atlantic (Haiti; USA), Hurricane *Matthew* Estimated economic losses US$ 10 billion; at least 546 deaths in Haiti and 49 in the United States
August 2017, North Atlantic (USA – Texas), Hurricane *Harvey* Estimated economic losses US$ 125 billion, 89 deaths
August–September 2017, North Atlantic (Caribbean; USA), Hurricane *Irma* Estimated economic losses US$ 57 billion, 134 deaths
September 2017, North Atlantic (Dominica; Puerto Rico), Hurricane *Maria* Estimated economic losses over US$ 90 billion; at least 140 deaths attributed directly to the storm but estimates of over 2 000 indirect deaths post-storm on Puerto Rico
March 2019, south-west Indian Ocean (Mozambique; Zimbabwe), Cyclones *Idai* and *Kenneth* At least 1 236 deaths attributed to Cyclone *Idai* – the most for a southern hemisphere cyclone for at least 100 years. *Kenneth* was more intense than *Idai* but made landfall in a sparsely populated area
Flood
June–July 2016, China – flood At least 310 deaths and US$ 14 billion in economic losses were attributed to the floods across the season
August 2017, India (north-east); Bangladesh; Nepal – flood At least 1 200 deaths were reported across the three countries, and 40 million people were affected in some way, with the spread of waterborne disease a significant factor
August 2017, Sierra Leone – landslide Major destruction and an estimated 1 102 death
June–July 2018, Japan – flood At least 245 deaths were reported, along with 6 767 houses destroyed.
August 2018, India (Kerala) – flood 1.4 million people were displaced and 5.4 million affected in some way. At least 223 deaths were reported, with economic losses estimated at US$ 4.3 billion

Storm and tornado

April 2016, USA – Texas – hailstorm
Estimated losses US$ 3.5 billion, amongst the highest known for a hailstorm in the United States

June 2016, China - tornado
At least 99 deaths were reported – one of the most destructive tornadoes in recorded Chinese history

May 2018, India (north) – severe windstorm, dust
At least 112 deaths were reported, mostly in Uttar Pradesh, from wind damage and poor air quality

June 2018, USA – Dallas, Denver – hailstorm
Losses were estimated at US$ 1.3 billion in Dallas-Fort Worth and US$ 2.2 billion in Denver

October 2018, Mediterranean (especially Italy; Slovenia; Croatia) – extratropical cyclone
Major wind damage and flooding in several countries; 30 deaths in Italy were attributed to the storm

Heatwave

May and June 2015, India; Pakistan – heatwave
2 248 deaths were reported due to the heat in India, and 1 229 in Pakistan

Summer 2015/16, South Africa – heatwave
There were numerous heatwaves in South Africa during the 2015/16 summer. Pretoria broke its previous record high temperature on three separate occasions

Summer 2015 and 2018, Europe – heatwaves
In France 3 275 and 1 500 excess deaths were attributed to the heat in 2015 and 2018, respectively

Summer 2018–19, Australia – heatwave
Hottest summer on record for Australia. There were also significant heatwaves in the 2016/17 and 2017/18 summers, especially in New South Wales

June–July 2019, Europe – heatwave
Two major long and extended heatwaves recorded in Europe in June–July 2019 with national records broken in many countries. In southern France a national record for any month of 46.0 °C was observed. The heat dome spread northwards through Scandinavia and towards Greenland where it accelerated the already above-average rate of ice melt

Drought

2015/16, Northwest South America; Central America; Caribbean – drought
Drought associated with the 2015/16 El Niño affected many parts of northern South America, Central America and the Caribbean. Rainfall averaged across the Amazon basin in Brazil in 2016 was the lowest on record

2015–2018, Africa – drought
Severely depleted water supply storages occurred in Cape Province of South Africa, leading to Cape Town to potentially run out of water during 2018. This followed severe drought in many parts of southern Africa in 2015 and 2016, following poor rainy seasons in 2014–2015 and 2015–2016. In east Africa in 2016–2017, 6.7 million people in Somalia were experiencing food insecurity at the drought's peak, decreasing to 5.4 million by the end of 2017 as conditions eased

2017–2019, Australia (mostly eastern) – drought
There were significant agricultural losses, as well as large-scale fish deaths after the Darling River ceased to flow

October 2017 – March 2018, northern Argentina; Uruguay – drought
There were heavy losses to summer crops with agricultural losses estimated at US$ 5.9 billion

2018, Europe (northern and central) – drought
There were heavy agricultural losses across numerous countries, and low flows in the Rhine severely disrupted river transport, causing significant economic losses

Wildfire

2015, Indonesia – wildfire
Drought led to extensive wildfires in Indonesia in the second half of 2015. 2.6 million hectares were reported to have burned. 34 deaths were directly attributed to the fires

May 2016, Canada (Alberta) – wildfire
A wildfire caused major damage in Fort McMurray, Alberta, in May. Insured losses exceeded US$ 3 billion with indirect losses of several billion dollars more

2016, 2019, Australia (Tasmania) – wildfire
Long-lived fires, associated with severe drought in normally wet areas. The fires burned World Heritage areas that are believed not to have experienced fire for at least several hundred years

July 2018, Greece – wildfire
Major fast-moving wildfires affected the region around Athens, driven by strong winds which reached 124 km/h. At least 99 deaths were reported, the heaviest loss of life in a wildfire globally since 2009

November 2018, USA (California) – wildfire
The town of Paradise was largely destroyed by a fast-moving wildfire. At least 85 lives were lost, and economic losses were estimated at US$ 16.5 billion, the largest on record for a wildfire globally

Cold event

February 2015, eastern USA and Canada – cold
Persistent cold in the north-east United States and eastern Canada. It was the second coldest February on record for the north-east region of the United States

January 2016, East Asia – cold
In late January, abnormally low temperatures extended south from eastern China as far south as Thailand. Guangzhou experienced its first snow since 1967 and Nanning its first since 1983

July 2017, Argentina – cold
Temperature at Bariloche, Argentina, fell to –25.4 °C on 16 July, 4.3 °C below the previous lowest on record

February–March 2018, Europe – cold/snow
Abnormal cold for late winter and early spring extended across much of Europe. Eastern Ireland had its heaviest snowfalls for more than 50 years with totals exceeding 50 cm in places

January–February 2019, north-central USA; interior western Canada – cold
Persistent very cold conditions in late January and February in the north-central United States and interior western areas of Canada

ATTRIBUTION OF EXTREME EVENTS

THE LIKELIHOOD OF OCCURRENCE OF HEATWAVES HAS BEEN SIGNIFICANTLY INCREASED BY ANTHROPOGENIC CLIMATE CHANGE

Determining the extent, if any, to which the chance of extreme events occurring has been affected by anthropogenic climate change is an active area of science, with hundreds of papers published in the last five years. Many of these studies appear one to two years after the event, but there is also an increasing interest in attribution of events relatively soon after the event, using already established methods.

According to recently published peer-reviewed studies in the annual supplement to the *Bulletin of the American Meteorological Society*, over the period 2015 to 2017, 62 of the 77 events reported show a significant anthropogenic influence on the event's occurrence, either directly, or indirectly (through, for example, influencing atmospheric circulation patterns that contributed to the event). Attribution studies are also published in other journals and reports.

Almost every study of a significant heatwave since 2015 has found that its probability has been significantly increased by anthropogenic climate change. For example, a study found that the heatwave that affected Japan in July 2018[11] would have been impossible without human influence. In general, the most clear-cut results are obtained for indicators that cover a large area over a substantial period of time (for example, a national mean monthly temperature), with more uncertainty for results at single locations over periods of a few days.

An increasing number of studies are also finding a human influence on the risk of extreme rainfall events, sometimes in conjunction with other major climate influences such as ENSO. One example is the extreme rainfall in eastern China in June–July 2016, where two studies[12] found that human influence significantly increased the risk of the event, with the signal less clear in a third

[11] Imada et al., 2019.

[12] Sun and Miao, 2018; Yuan et al., 2018.

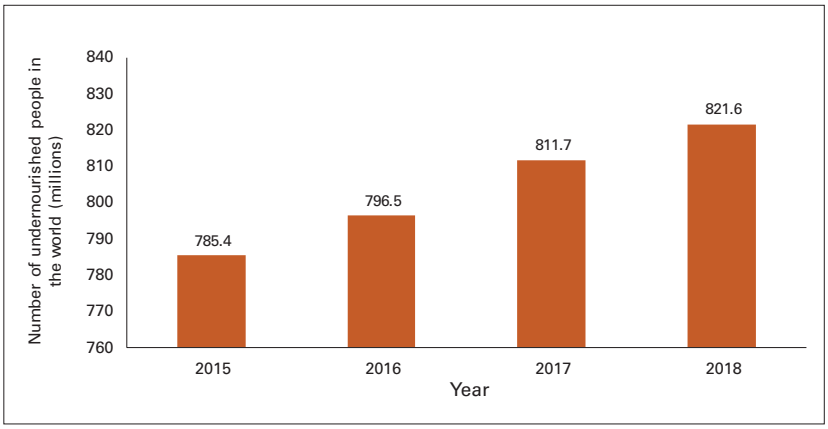

Figure 20. Number of undernourished people in the world, 2015–2018. *Source: FAO, International Fund for Agricultural Development (IFAD), United Nations Children's Fund (UNICEF), World Food Programme (WFP) and World Health Organization (WHO), 2019*

study.[13] Some, although not all, droughts also show a direct or indirect human influence, such as the 2016/17 East African drought,[14] which was strongly influenced by warm sea-surface temperatures in the western Indian Ocean to which human influence contributed.

Very few studies have yet found any human signal in small-scale severe weather events such as thunderstorms and tornadoes, and the limited studies of anthropogenic influence on fire weather, such as the February 2017[15] event in New South Wales, Australia, have mostly been inconclusive. While few clear anthropogenic signals have been found in tropical cyclone intensity and frequency, it has been found that human influences have increased the amount of rainfall associated with tropical cyclones. In one notable example, Hurricane *Harvey* in the Houston area in 2017, a study concluded that human influence increased the amount of rainfall that occurred by about 15% (8% to 19%).[16]

HIGHLIGHTS ON PROMINENT CLIMATE-RELATED RISKS

RECENT RISE IN FOOD INSECURITY AND GLOBAL HUNGER DUE TO DROUGHT IMPACT

According to the Food and Agriculture Organization (FAO) annual reports, *The State of Food Security and Nutrition in the World*, climate variability and extremes are among the key drivers behind the recent rises in global hunger and one of the leading causes of severe food crises (Figure 20). The changing nature of climate variability and extremes is negatively affecting all dimensions of food security (food availability, access, utilization and stability).

The impact of the 2015–2016 El Niño on agricultural vegetation is clearly visible through the frequency of drought conditions in 2015–2017. The map in Figure 21 shows that large areas in Africa, parts of central America,

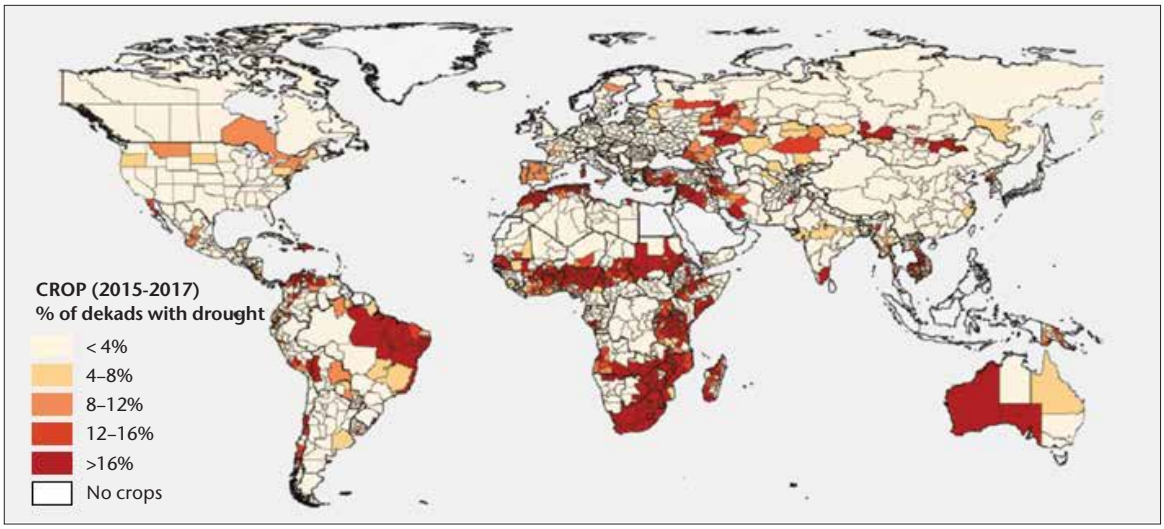

Figure 21. Percentage of time (dekad is a 10-day period) with active vegetation when the anomaly hot spots of agricultural production (ASAP) was signalling possible agricultural production anomalies according to the Normalized Difference Vegetation Index (NDVI) for more than 25% of the crop areas in 2015–2017. *Source: FAO, IFAD, UNICEF, WFP and WHO, 2018*

[13] Zhou et al., 2018.

[14] Funk et al., 2019.

[15] Hope et al., 2017.

[16] Hope et al., 2017.

Brazil and the Caribbean, as well as Australia and parts of the Near East experienced a large increase in frequency of drought conditions in 2015–2017 compared to the 14-year average.

The risk of food insecurity and malnutrition is greater nowadays because livelihoods and livelihood assets – especially of the poor – are more exposed and vulnerable to changing climate variability and extremes. In the Horn of Africa, rainfall deficits led to the failure of the 2016 and 2017 rainy seasons and the number of food-insecure people rose significantly in Eastern Africa. In Somalia, more than half of the cropland was affected by drought, and herds had reduced by 40% to 60% due to increased mortality and distress sales. In Malawi, the 2015 floods resulted in severe losses to crops, livestock, fisheries and forestry assets, and production flows. According to the United Nations High Commissioner for Refugees Protection and Return Monitoring Network, some 883 000 new internal displacements were recorded between January and December 2018, with conflict the primary reason for displacement (36%), followed by flooding (32%) and drought (29%). As at September 2018, up to 200 000 of the total estimated 900 000 Rohingya refugees were exposed to these natural hazards.

THE OVERALL RISK OF CLIMATE-RELATED ILLNESS OR DEATH HAS INCREASED

Based on WHO data and analysis, the overall risk of heat-related illness or death has climbed steadily since 1980, with around 30% of the world's population now living in climatic conditions that deliver potentially deadly temperatures at least 20 days a year.

Other climate-related events such as heavy rain and associated floods create favourable conditions for various sorts of epidemic outbreaks. In cholera-endemic countries, an estimated 1.3 billion people are at risk, while in Africa alone about 40 million people live in cholera "hotspots". WHO has recognized that large cholera outbreaks in eastern and central, and later southern Africa were likely enhanced by El Niño-driven weather conditions, in particular extreme rainfall and floods. Flood events are also often associated with outbreaks of water-borne diseases or those linked to poor sanitation, as was reported in Bangladesh during the August 2017 floods.

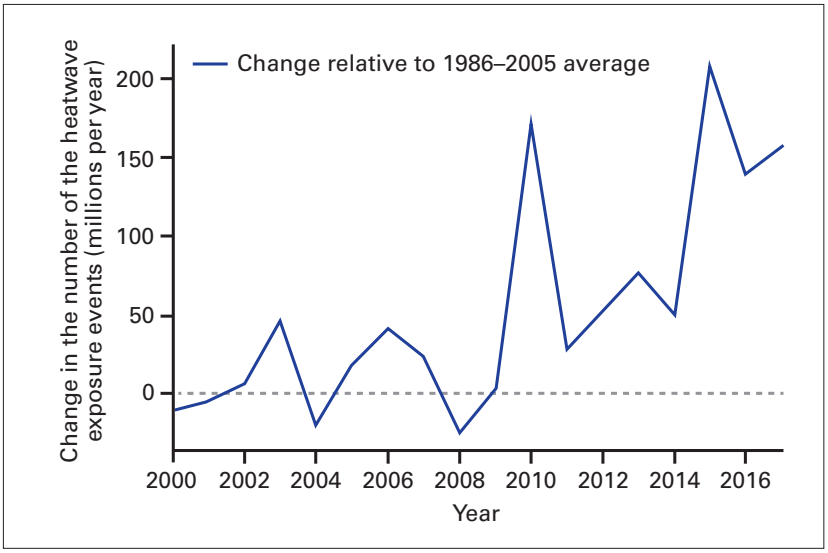

Figure 21. The change in the number of people exposed to heatwaves in millions per year from 2000 to 2017, relative to the 1986–2005 average. *Source: Watts et al., 2018*

MARINE LIFE AND ECOSYSTEMS ARE BEING THREATENED BY HIGHER SEA-SURFACE TEMPERATURES

According to IOC-UNESCO, significantly higher sea-surface temperatures, as much as 3 °C above average in some areas, are implicated in dramatic changes to the physical, chemical and biological state of the marine environment, with great impacts on food chains and marine ecosystems, as well as socioeconomically important fisheries. Among the areas significantly affected are the Great Barrier Reef off the east coast of Australia, Pacific island countries such as Fiji and Kiribati, and the Okinawa region of Japan. Coral mortality of up to 50% to 70% has been reported.

IOC-UNESCO also reported that oxygen is declining in the open and coastal oceans, including estuaries and semi-enclosed seas. Since the middle of the last century, there has been an estimated 1%–2% decrease in the global ocean oxygen inventory. Regions with historically low oxygen concentrations are expanding, and new regions are now exhibiting low oxygen conditions. Global warming is expected to contribute to this decrease directly because the solubility of oxygen decreases in warmer waters,

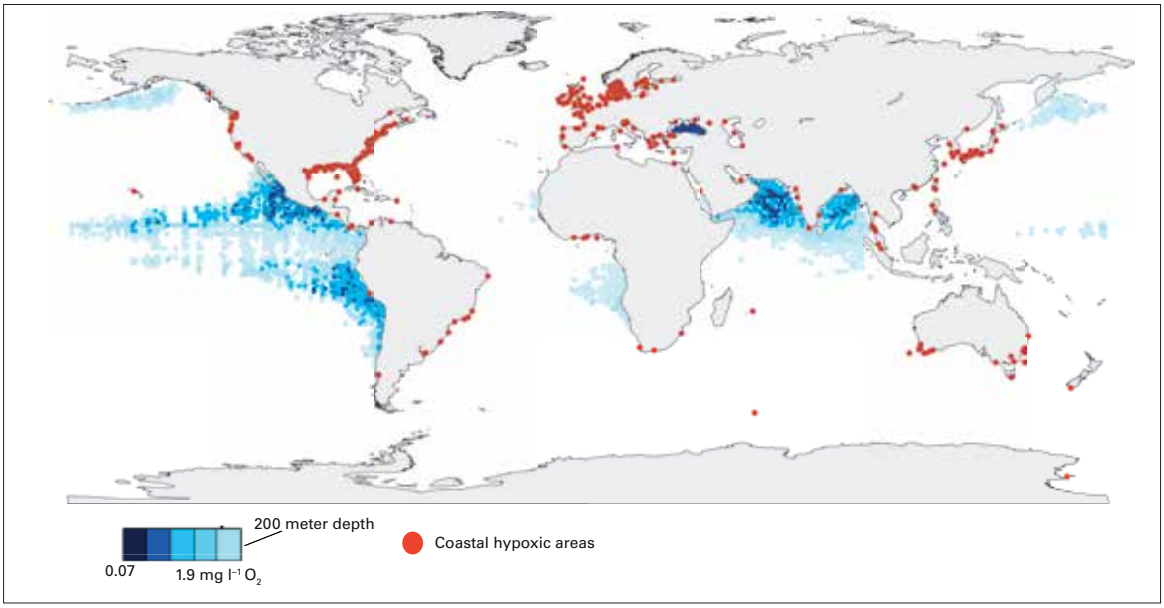

Figure 23. Oxygen minimum zones (blue) and areas with coastal hypoxia (red) in the world's oceans. Coastal hypoxic sites mapped here are systems where oxygen concentrations of < 2 mg/L have been recorded and in which anthropogenic nutrients are a major cause of oxygen decline. *Sources: data from Diaz and Rosenberg (2008), figure adapted after Breitburg et al., 2018*

and indirectly through changes in ocean dynamics that reduce ocean ventilation, which is the introduction of oxygen to the ocean interior.

GROSS DOMESTIC PRODUCT IS FALLING IN DEVELOPING COUNTRIES DUE TO INCREASING TEMPERATURES

The International Monetary Fund found that for a median- and low-income developing country, with an annual average temperature of 25 °C, the effect of a 1 °C increase in temperature leads to a growth decrease of 1.2%. Countries whose economies are projected to be significantly adversely affected by an increase in temperature produced only about 20% of global GDP in 2016; however, they are currently home to nearly 60% of the global population and are projected to be home to more than 75% by the end of the century.

REFERENCES

Breitburg, B., L.A. Levin, A. Oschlies, M. Grégoire, F.P. Chavez, D.J. Conley, V. Garçon, D. Gilbert, D. Gutiérrez, K. Isensee, G.S. Jacinto, K.E. Limburg, I. Montes, S.W.A. Naqvi, G.C. Pitcher, N.N. Rabalais, M.R. Roman, K.A. Rose, B.A. Seibel, M. Telszewski, M. Yasuhara and J. Zhang, 2018: Declining oxygen in the global ocean and coastal waters. IOC Global Ocean Oxygen Network. *Science*, 359(6371), https://doi.org/10.1126/science.aam7240.

Brown, R.D., B. Brasnett and D. Robinson, 2003: Gridded North American monthly snow depth and snow water equivalent for GCM evaluation. *Atmosphere-Ocean*, 41(1):1–14, https://doi.org/10.3137/ao.410101.

Brun, E., V. Vionnet, A. Boone, B. Decharme, Y. Peings, R. Valette, F. Karbou and S. Morin, 2013: Simulation of Northern Eurasian local snow depth, mass, and density using a detailed snowpack model and meteorological reanalyses. *Journal of Hydrometeorology*, 14: 203–219, https://doi.org/10.1175/JHM-D-12-012.1.

Cheng, L., et al., 2019: 2018 Continues record global ocean warming, *Advances in Atmospheric Sciences*, 36:249–252, https://doi.org/10.1007/s00376-019-8276-x.

Estilow, T.W., A.H. Young and D.A. Robinson, 2015: A long-term northern hemisphere snow cover extent data record for climate studies and monitoring. *Earth System Science Data*, 7:137-142, https://doi.org/10.5194/essd-7-137-2015.

Fetterer, F., K. Knowles, W.N. Meier, M. Savoie and A.K. Windnagel, 2017: Sea Ice Index, Version 3. National Snow and Ice Data Center, https://doi.org/10.7265/N5K072F8.

Funk, C., D. Pedreros, S. Nicholson, A. Hoell, D. Korecha, G. Galu, G. Artan, Z. Segele, A. Tadege, Z. Atheru, F. Teshome, K. Hailermariam, L. Harrison and C. Pomposi, 2019: Examining the potential contributions of extreme "western V"

sea surface temperatures to the 2017 March-June east African drought. *Bulletin of the American Meteorological Society*, 100:S55-S60, https://doi.org/10.1175/BAMS-D-18-0108.1.

Hope, P., M.T. Black, E. Lim, A. Dowdy, G. Wang, R.J. Fawcett and A.S. Pepler, 2019: On determining the impact of increasing atmospheric CO2 on the record fire weather in eastern Australia in February 2017. *Bulletin of the American Meteorological Society*, 100:S111-116, https://doi.org/10.1175/BAMS-D-18-0135.1.

Imada, Y., M. Watanabe, H. Kawase, H. Shiogama and M. Arai, 2019: The July 2018 high temperature event in Japan could not have happened without human-induced global warming. *Scientific Online Letters on the Atmosphere*, 15A:8–12, https://doi.org/10.2151/sola.15A-002.

Oldenborgh, G.J. van, K. van der Wiel, A. Sebastian, R. Singh, J. Arrighi, F. Otto, K. Haustein, S. Li, G. Vecchi and H. Cullen, 2017: Attribution of extreme rainfall from Hurricane Harvey, August 2017. *Environmental Research Letters*, 12(12):124009, https://doi.org/10.1088/1748-9326/aa9ef2.

Reichle, R.H., C.S. Draper, Q. Liu, M. Girotto, S.P. Mahanama, R.D. Koster and G.J. De Lannoy, 2017: Assessment of MERRA-2 land surface hydrology estimates. *Journal of Climate*, 30:2937–2960, https://doi.org/10.1175/JCLI-D-16-0720.1.

Sun, Q. and C. Miao, 2018: Extreme rainfall (R20mm, RX5Day) in Yangtze-Huai, China, in June-July 2016: the role of ENSO and anthropogenic climate change. *Bulletin of the American Meteorological Society*, 99:S102-S106, https://doi.org/10.1175/BAMS-D-17-0091.1.

Takala, M., K. Luojus, J. Pulliainen, C. Derksen, J. Lemmetyinen, J.-P. Kärnä, J. Koskinen and B. Bojkov, 2011: Estimating northern hemisphere snow water equivalent for climate research through assimilation of space-borne radiometer data and ground-based measurements. Remote Sensing of *Environment*, 115(12):3517–3529, https://doi.org/10.1016/j.rse.2011.08.014.

Watts, N., et al., 2018: The 2018 report of The Lancet Countdown on health and climate change: shaping the health of nations for centuries to come, *Lancet*, 392(10163):2479–2514, https://doi.org/10.1016/S0140-6736(18)32594-7.

Yuan, X., S. Wang and Z. Hu, 2018: Do climate change and El Niño increase likelihood of Yangtze River rainfall? *Bulletin of the American Meteorological Society*, 99:S113–S117, https://doi.org/10.1175/BAMS-D-17-0089.1.

Zemp, M., M. Huss, E. Thibert, N. Eckert, R. McNabb, J. Huber, M. Barandun, H. Machguth, S. U. Nussbaumer, I. Gärtner-Roer, L. Thomson, F. Paul, F. Maussion, S. Kutuzov and J.G. Cogley, 2019: Global glacier mass changes and their contributions to sea-level rise from 1961 to 2016. *Nature*, 568(7752), 382–386, https://doi.org/10.1038/s41586-019-1071-0.

Zhou, C., K. Wang and D. Qi, 2018. Attribution of the July 2016 extreme precipitation event over China's Wuhan. *Bulletin of the American Meteorological Society*, 99:S107–S112, https://doi.org/10.1175/BAMS-D-17-0090.1.

For more information, please contact:

World Meteorological Organization

7 bis, avenue de la Paix – P.O. Box 2300 – CH 1211 Geneva 2 – Switzerland

Communication and Public Affairs Office

Tel.: +41 (0) 22 730 83 14/15 – Fax: +41 (0) 22 730 80 27

Email: cpa@wmo.int

public.wmo.int

JN 191303